Proceedings of the 20th International Conference on Soil Mechanics and Geotechnical Engineering– Rahman and Jaksa (Eds)

Oedometric-continuous corrected law for the stress-strain relationship of soils under shallow foundations

Loi corrigée œdométrique-continue pour la relation contrainte-déformation des sols sous fondations peu profondes

Wagdi Naime Yehia

Highway Engineering Department, Central University of Venezuela, Los Chaguaramos, Caracas, Venezuela and Doctoral Program in Applied Sciences, University of Los Andes, Mérida, Venezuela, wagdin@gmail.com

ABSTRACT: Oedometric Continuous law is an alternative to the conventional law currently used to interpret oedometric behavior. It is expressed through continuous equations that can be derived and integrated throughout all practical stress domain, for both, normally consolidated and overconsolidated soils. Considering stress paths starting from ko line, of the oedometric behaviour, tending towards k_f line, of the stress limit state, there are equations developed to modify the oedometric analysis into horizontal strains on the soil, generating a new stress-strain law that better fits real behavior under shallow foundations. The new law is called Oedometric-Continuous Corrected Law. This law considers a parabolic function scaling on to the horizontal strains in extension with gradual reduction of the horizontal stress with respect to the oedometric condition. In this research we assume a linear path, similar but not coincident to the lineal path that is obtained by elasticity equations. The new method was used to verify the settlement calculation, the vertical deformation profile and the horizontal displacements profile on an embankment over very soft marine clays of Muar (Indonesia) and on a large spread footing over medium dense sandy soil in Texas (USA), obtaining great correspondence with the measured results.

RÉSUMÉ : La loi oedométrique-continue est une alternative à la loi traditionnelle pour l'interprétation du comportement oedométrique des sols, en indiquant que l'avantage s'exprime à travers des équations continues, dérivables et intégrables dans tout le domaine des contraintes pratiques, parlant soit si le sol est normalement consolidé, soit préconsolidé. Par la prise en compte d'un chemin de contraintes partant de la ligne Ko, du comportement oedométrique, de la tendance vers la ligne de Kf, de l'état limite de contrainte, on développe des expressions qui modifient les équations du comportement oedométrique avec les déformations horizontales sur le sol, générant une nouvelle loi contrainte-déformation qui s'adapte mieux au comportement réel sous fondations peu profondes. La nouvelle loi est appelée loi corrigée œdométrique-continue. Cette loi fonde son développement sur une croissance parabolique des déformations horizontales unitaires en extension avec réduction progressive de la contrainte horizontale par rapport à la condition oedométrique. L'écart des contraintes horizontales par rapport à la condition oedométrique dépendra de la trajectoire des contraintes. Dans cette recherche, nous supposons un chemin linéaire, probablement mais non coïncident avec le chemin linéaire obtenu en considérant les équations de Boussinesq. La nouvelle méthode a été utilisée pour vérifier le calcul du tassement et du profil de déplacements horizontaux sur un remblai dans les argiles molles de Muar (Indonésie) et du profil de déformation verticale unitaire sur une fondation peu profonde sur des sables au Texas (USA), obtenant ainsi une grande correspondance avec les résultats mesurés.

KEYWORDS: Compressibility, oedometric strain, horizontal deformation, shallow foundations, stress path, stress-strain relationship.

1 INTRODUCTION.

The current oedometric conventional method considers the compressibility characteristics of soils, represented by the following variables: (1) the initial void ratio (e_o), (2) the precompression pressure (σ_m), (3) the recompression and the compression indexes (Cr and Cc), which are defined as the slopes of assumed straight lines on the two first zones of the *e-log(σ)* compressibility curve, and (4) the coefficient of volume compressibility (m_v), which is the inverse of the oedometric modulus (Es), that is defined as the stress-strain curve slope. All of these are included in Figure 1. For almost a century the conventional oedometric method has been widely used to primary consolidation settlements estimates on shallow foundations, see e.g.: Skempton, Peck, & MacDonald (1955), Peck & Uyanik (1955), Wijemunige & Moh (1989), Balasubramaniam, Cai, Zhu, Surarak, & Oh (2010), Yune & Olgun (2016), Indraratna, Zhong, Fox, & Rujikiatkamjorn (2017) and Chen, Gao, Elsayed, & Yang (2019).

The compressibility curve in semi log scale is the most common method used worldwide to interpret soil compression characteristics. This gives as a result an S-shaped inverse curve, as depicted in Figure 1, (Schmertman, 1953; Vesic & Clough, 1968; Butterfield 1979; Nagaraj, Murthy, Vatsala, & Joshi, 1990; Zheng, Hryciw, & Ventola, 2017; Carneiro, Gerscovich, & Danziger, 2018). Pre-consolidated and normally consolidated domains are separated by the precompression stress, covering the practical application domain for settlements calculation. Starting with the transition pressure σt, axial stiffness increses meanwhile void ratio approaches to its minimum value. In the final domain the soil behaviour is similar to the remoulded soil.

The e-log(σ) curve is highly nonlinear and it is not appropriate to be defined by simple Cr and Cc values. The oedometric modulus strongly depends on pressure level. If it is assumed that Cc and Cr are constants, then one can obtain the non-continuous equations on σm. Published experimental results reveal that the compressibility equations could be curved and continuous. Sridharan & Gurtug (2005) show a clear variation of the slope Cc in the compressibility curve versus axial pressure. Mesri & Choi (1985) proposed a modified compression index C´c, which is the slope of the lines connecting the M point (figure 1) with different points on the compression curve from σ_p.

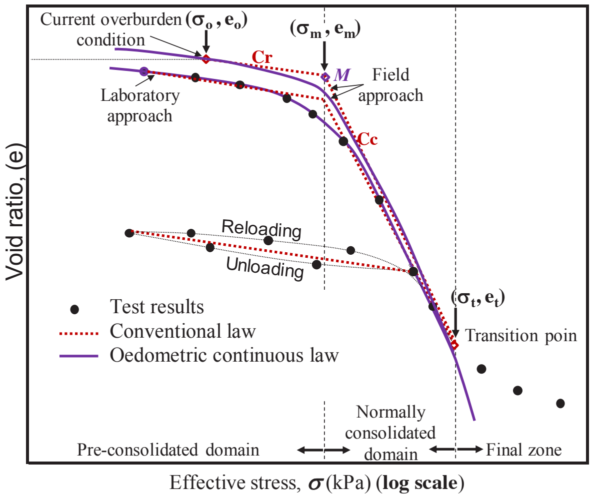

Figure 1. A typical e-log(σ) compressibility curve. Oedometric conventional and oedometric continuous laws

The equation (1) shows the main relationships of the conventional oedometric law, where ε_m is the vertical strain at the precompression stress.

$$
\begin{cases}
E_s = \frac{ln(10)(1+e_o)}{C_{c/r}}\sigma \rightarrow C_r \ if\ \sigma \leq \sigma_m \ and\ C_c \ if\ \sigma > \sigma_m & (a) \\
\varepsilon = \frac{C_r}{1+e_o} log(\sigma/\sigma_o) \rightarrow \sigma \leq \sigma_m & (b.1) \\
\varepsilon = \varepsilon_m + \frac{C_c}{1+e_o} log(\sigma/\sigma_m) \rightarrow \sigma > \sigma_m & (b.2) \\
e = e_o + C_r\, log(\sigma/\sigma_o) \rightarrow \sigma_o \leq \sigma \leq \sigma_m & (c.1) \\
e = e_m + C_c\, log(\sigma/\sigma_m) \rightarrow \sigma_m < \sigma \leq \sigma_t & (c.2)
\end{cases} \quad (1)
$$

The oedometric-continuous law (Naime W. , 2019) is supported on analysis of the oedometric modulus variation versus effective axial stress, suggested previously by Janbu (1963 and 1969), Wissa, Christian, Davis, & Heiberg (1971), Stamatopoulos & Kotzias (1973 and 1978), Papadopoulos (1992) and Naime (2003). Based on the hypothesis that the oedometric modulus increases linearly with the effective axial stress, starting from an initial value (Eso) and a linear approach, the continuous equations were developed, with a high correlation in the first two zones of the compressibility curve and the oedometric stress-strain relationship. Analysis of several oedometric tests on soils, ranging from low to high compressibility, showed that the oedometric-continuous law is better adapted to the experimental results than the conventional method (Naime, 2019). Equation (2) shows the main relationships between the linear approach and the oedometric-continuous law, where Es and λ are constants.

$$
\begin{cases}
E_s = E_{so} + \lambda\sigma & (a) \\
\varepsilon = \frac{1}{\lambda} ln\left(\frac{E_{so}+\lambda\sigma}{E_{so}}\right) \longrightarrow \forall\, \sigma \leq \sigma_t & (b) \\
e = e_o - C_{ce}\, log\left(1 + \frac{\lambda}{E_{so}}\sigma\right) \longrightarrow \forall\, \sigma \leq \sigma_t & (c) \\
C_{ce} = \frac{ln(10)(1+e_o)}{\lambda} &
\end{cases} \quad (2)
$$

Oedometric-continuous equations can be differentiable within the practical application domain, thus it can be used for advanced numerical simulations and are ideal to superimpose effects that complement the oedometric behaviour, e.g., the effects of the horizontal deformations.

It is worth mentioning that below shallow foundations the soil presents horizontal deformations. This has been supported by real-scale load test, see e.g: Eggestad (1964), Loganathan, Balasubramaniam, & Bergado (1993), Da Fonseca, Fernandes, & Cardoso (1997), Wijemunige & Moh (1989) and Briaud & Gibbens (1999). As the conventional oedometric criterion does not admit horizontal deformations it is less accurate than the axial effective stress increases. For normal design conditions, comparing the oedometric settlement calculations with the real measured values, one can note that the oedometric criterion underestimates the settlement with deficits ranging between 13% and 22% (Skempton, Peck, & MacDonald 1955; Peck & Uyanik 1955; Pitt 1981; Chen, Gao, Elsayed, & Yang 2019; Naime, 2019).

In this research work, a modification to the stress-strain equation of the linear approach to the continuous oedometric law is presented, adding up the horizontal deformations effect. In this way, a better model adapted to the real behaviour of soils under shallow foundations is obtained which allows better estimates of settlements and soil deformations in general.

2 OEDOMETRIC-CONTINUOUS CORRECTED LAW (OCCL)

Figure 2 presents the theoretical correlations among different linear stress paths with axisymmetric conditions and the expected horizontal deformations. The oedometric stress path follows the ko line (A→D), without horizontal deformations. Any path below ko line will lead to horizontal compression deformations, e.g., the isotropic compression path (A→B) or the general one (A→C). Any path above ko line will lead to horizontal deformations (extension) like the general case (A→E) or the limit imposed by the k=0 line, representing the shearing stage of a consolidated-drained test (A→F).

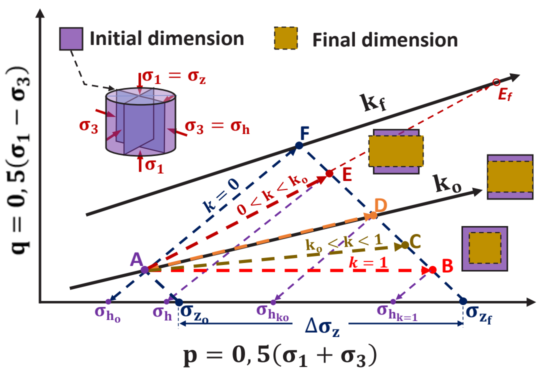

Figure 1. Theoretical correlations among stress path with axisymmetric conditions and lateral deformations on the soil.

These stress paths represent a vertical stress increase $\Delta\sigma z$ starting from vertical and horizontal initial stresses σ_{z_o} and σ_{h_o} The horizontal deformation is conditioned by the final horizontal stress: at the right side of $\sigma_{h_{ko}}$ a horizontal compression will appear and at the left side a horizontal extension. Under a shallow foundation, the final horizontal stress σh will be between σ_{h_o} and $\sigma_{h_{ko}}$ just as the A→E path, which when $\Delta\sigma z$ increases it could be projected to failure at the point E_f, see figure 2.

The linear approach of the oedometric-continuous law (equation 2b) is modified to consider a linear stress path such A→E, increasing the vertical deformation due to horizontal extension.

The hypotheses are as follows:

1) The final horizontal stress has an intermediate value between σ_{h_o} and $\sigma_{h_{ko}}$:

$$\sigma_h = k_o\left(\sigma_{z_o} + \eta\Delta\sigma_z\right) \tag{3}$$

The η value pin points the horizontal stress to be between the indicated limits. If $\eta = ½$, σ_h is the midpoint, $\eta = 0$ or $\eta = 1$ represent either the conditions of the shearing stage of a consolidate-drained test or the oedometric test respectively (σ_h is σ_{h_o} or $\sigma_{h_{ko}}$). Stress path can intercept the k_f line if $\eta k_o < tan^2(45 - \phi/2)$, where ϕ is the effective friction angle.

2) The volumetric deformation is equivalent to the oedometric one. For small deformations, equation (4) shows the vertical strain correction (the compression is positive), where ε_{oe} is the oedometric strain and ε_h is the horizontal strain.

$$\varepsilon_z = \varepsilon_{oe} - 2\varepsilon_h \tag{4}$$

3) In the relationship between the horizontal deformation and the coefficient of absolute lateral pressure (k), the extension path is equivalent to a parabolic curve shown in Figure 3. Thus, equation (5) presents the horizontal deformation varying from the initial rest state ($\varepsilon_h = 0$) to the horizontal deformation at failure (ε_{hf}) where k is reduced from ko to ka.

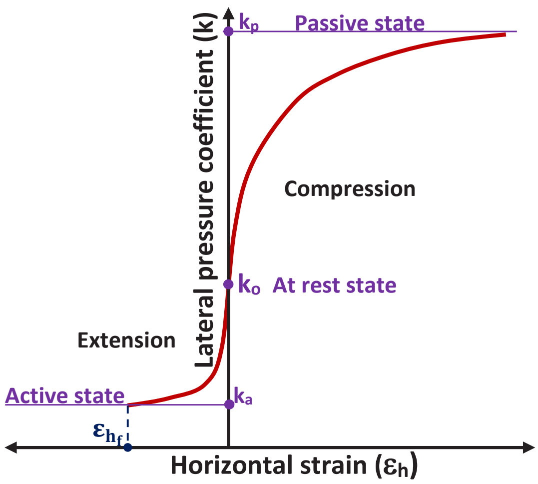

Figure 3. Relationship between horizontal strain and lateral pressure coefficient

$$\frac{\varepsilon_h}{\varepsilon_{h_f}} = \sqrt{1 - \frac{k_o - k}{k_o - k_a}} - 1 \tag{5}$$

Making substitutions and algebraic modifications in equation (5), based on equation (4), equation (6) is obtained which represents the vertical strain equation of the oedometric-continuous corrected law. For any depth (*z*), ε_z is the vertical strain, $\Delta\sigma_z$ is the vertical effective stress increment, σ_{zo} is the initial vertical effective stress, ε_{hf} is the horizontal strain at failure, σ_z is the final vertical effective stress and σ_{zf} is the effective vertical stress that produces the failure to the respective stress path, according to the Mohr-Coulomb criterion. Figure 4 shows the application of equation (6) for Guayana City's silty clay (Naime W. , 2019) at z = 0.75 m depth. The curve determined with stress path obtained by the elasticity equations is also presented, representing theoretically the stress path method (Lambe & Marr, 1979)

$$\varepsilon_z = \frac{1}{\lambda} ln\left[1 + \frac{\lambda\Delta\sigma_z}{E_{so} + \lambda\sigma_{oz}}\right] + 2\varepsilon_{h_f}\left(\sqrt{1 - \frac{\Delta\sigma_z}{\sigma_{z_f} - \sigma_{oz}}} - 1\right) \tag{6}$$

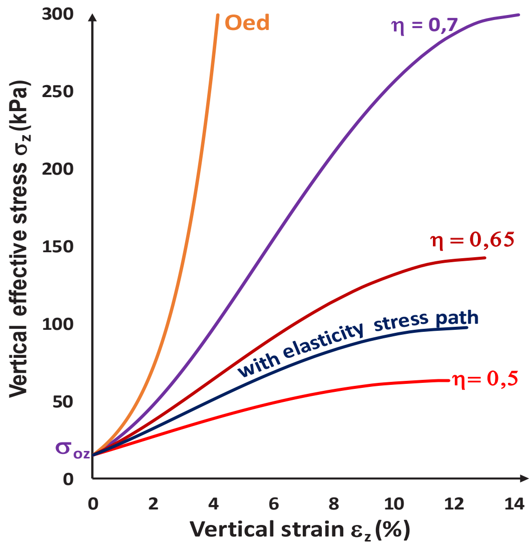

Figure 4. Vertical stress–strain relationship by the oedometric-continuous corrected law. Guayana City's silty clay at z= 0.75 m depth.

3 APPLICATION FOR SHALLOW FOUNDATIONS

Elastic solutions, like Bousinesq integrated equation, are used to determine the vertical stress increment $\Delta\sigma_z$. Equation (3) is used to determine the increase in horizontal stress due to $\Delta\sigma_z$. Under shallow foundations, the horizontal confinement increases due to the roughness of the soil-foundation contact, for example in Figure 5 which shows it schematically for the foundation axis, which also can be determined at any depth at x distance off the axis.

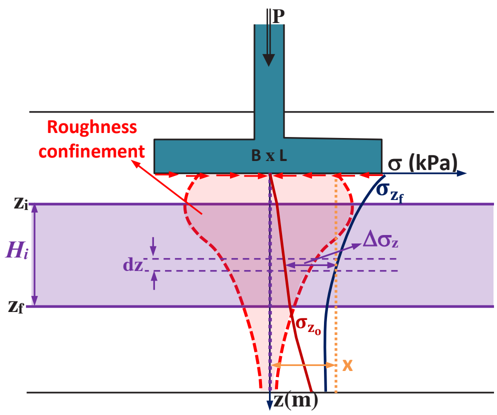

Figure 5. Stress increase below the center of a shallow foundation.

In this article, the roughness between foundation bottom and soil is treated as an additional increase of the horizontal stress. This increases the vertical effective failure stress σ_{zf}, and reduces the horizontal deformations obtained by equation (6). At the soil-foundation contact the induced horizontal stress is large and decreases with depth. In spite of considering a constant vale for η, the stress paths at different depths are not parallel and have a higher inclination as depth increases, due to the scarce increment in the horizontal stress resulting from of roughness. This effect is similar, but not the same, to the one obtained by determining the stress paths based on the elasticity equations for an increase in vertical stress without the roughness effect. The proposed procedure includes the roughness effect on deformations, and on the bearing capacity of shallow foundations.

4 MATERIALS AND METHOD

Two full scale test cases were analysed, first, a large spread footing load test (B = 3m) on medium dense silty sandy soil (Briaud & Gibbens, 1997), with measured vertical strain profile in the foundation axis, which was considered comparable with the continuous-oedometric corrected law. The second case was a large-scale field trial embankment constructed in 1988 over a very soft marine clay deposit located at a section of the express highway. The embankment was constructed at Muar flat in the valley of the Muar River by the Malaysian Highway Authority. This case was considered to compare both, the settlement measured at the center and the variation in percentage settlement with depth with respect to those settlements determined by the proposed method. In both cases, the profiles of horizontal displacements at the edge of the foundation were also analysed. The horizontal stress factor used wag $\eta = 0.5$. Numerical methods were used to integrate the equations, applying the Romberg method (R9) for settlements and Simpson's rule for horizontal displacements. The plastic deformations increase was determined with constant stress-strain slope at failure (derivative of the equation 6). The geotechnical profiles are summarized in Tables 1 and 2.

Table 1. Geotechnical parameters used for the sandy profile.

Depth m	γ kN/m³	ϕ'	C′ kPa	ε_{hf} %	ko	Eso kPa	λ
0-10	15,5	37	3	2	0,44	32.000	10
> 10	17,0	35	40	1	0,65	55.000	40

Table 2. Geotechnical parameters used for Muar profile.

Depth m	γ kN/m³	ϕ'	C′ kPa	ε_{hf} %	ko	Eso kPa	λ
0-1,5	15	12	8	7	0,8	2000	15
1,5-6,5	14	10	10	7	0,8	280	1,5
6,5-22,5	16	17	18	7	0,9	1700	10

5 RESULTS AND DISCUSSION

5.1 *Large spread footing load tests on sandy soil*

Five large spread footing load tests on sand were performed on the Texas A&M University National Geotechnical experimentation Site (Briaud & Gibbens, 1997, 1999). The square footings varied from 1 m to 3 m width and were loaded until the settlement reached 150 mm. The stratigraphic profile data can be reviewed in Briaud & Gibbens (1997).The upper soil, to a depth of 11 m, is a medium dense silty fine silica sand lightly overconsolidated. About 1 m was removed of overburden at the location of the spread footing tests. Below the sand layer there was a very hard dark gray clay layer which extends to a depth of at least 33 m. The water table is located at 5.9 m deep. In this article, one of the 3-m wide footings was analysed by calibrating the OCCL to achieve the 150 mm settlement with a vertical load of 8900 kN, as occurred in the real test. Table 1 summarizes the geotechnical parameters used in this article. Figure 6 shows the normalized vertical strains profile and the normalized lateral deformations profile, with S_{top} as the maximum settlement. A very good fit between the measured results with those calculated with the OCCL is observed.

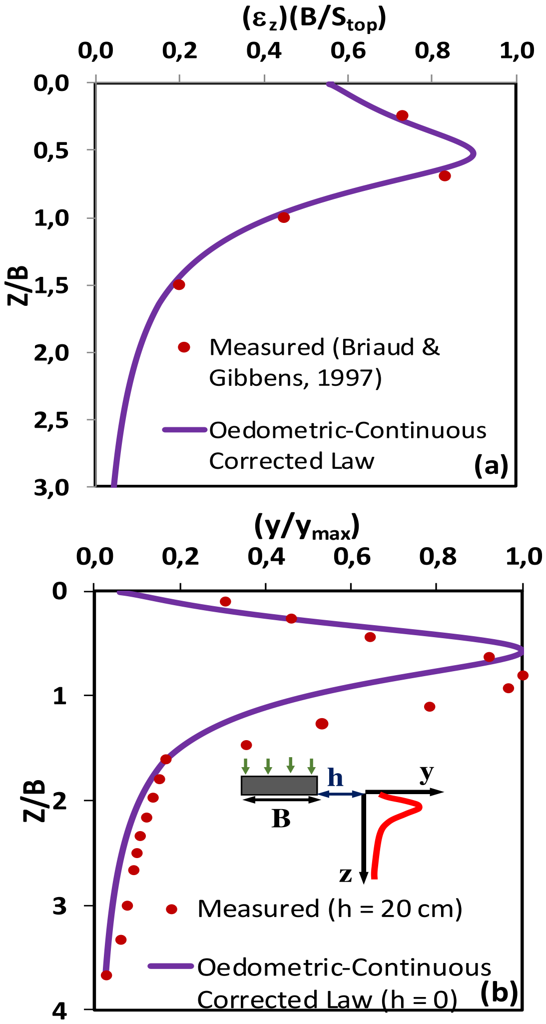

Figure 6. (a) Vertical strains profile. (b) Variation of ratio of lateral deformation to maximum lateral deformation with depth for 3 m square footing on sandy soil.

5.2 *Full scale trial embankment test on very soft Muar marine clay*

In 1988, the Malaysian Highway Authority was authorized to build a 13 full-scale test embankments at a section of the express highway located at Muar Flat in the valley of the Muar River. Two of such embankments were constructed without any ground improvement, one was 6 m high (171 m x 50 m in plan) and the other one was 3 m high (50 m x 32 m in plan). The program included the installation of various instruments to monitor the field performance. In this article it was considered the 3 m high embankment.

The stratigraphic profile data and the complete soil properties of Malaysian Muar clay were summarized by Brand and Premchitt (1989). There is a weathered crust of about 2 m thick above a 16 m thick layer of soft silty clay, divided into an upper very soft (5 m) and a lower soft silty clay (11 m). Immediately beneath this lower clay layer is a 0.3-0.5 m thick peaty soil followed by a stiff sandy clay. The clayey succession ends at a dense sand layer at about 22.5 m below ground level. The water table was 0.8 m deep. Table 2 summarizes the geotechnical parameters used in this article. The parameters of the OCCL model were determined using back-calculation based on the compressibility parameters reported by Brand and Premchitt (1989). The measurements results used in this work were taken from Balasubramaniam, et al. (2007).

The field consolidation curve had reported 105.5 cm settlement at 605 days on the embankment centre. The total measured settlement is 187 cm. By integrating equation (6) with respect depth, the calculated settlement is 187.6 cm. Figure 7a shows settlement profiles with respect to depth. The normalised lateral deformations are presented in figure 7b. The vertical deformation analysis was faithfully reflected by the proposed method with a very good settlement estimate.

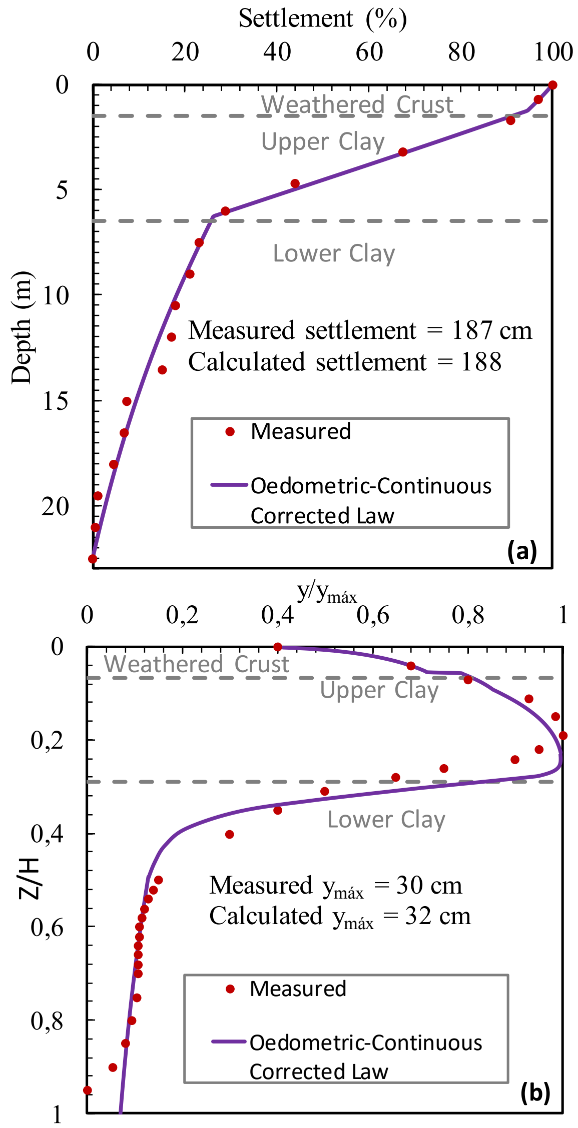

Figure 7 (a) Variation of percentage settlement with depth. (b) Variation of ratio of lateral deformation to maximum lateral deformation with depth for 3 m high Muar embankment.

The results show that the OCCL is an effective criterion for soil deformations analysis under shallow foundations. The vertical strain profile on sand is practically equivalent to that reported by Schmertmann, Hartman, & Brown (1978). The horizontal displacement profiles obtained for both case studies shows the same trend reported by several authors such as Eggstad (1964), Tavenas, Mieussens, & Bourges (1979), Tavenas & Leroueil (1980), Loganathan, Balasubramaniam, & Bergado (1993), Indraratna, Balasubramaniam, & Sivaneswaran (1997), Da Fonseca, Fernandes, & Cardoso (1997) and Naime (2019).

6 CONCLUSIONS

The analysis of deformations in shallow foundations must consider lateral deformations since settlements are affected by horizontal displacements. The oedometric-continuous corrected law superimposes the horizontal deformations effect on the vertical oedometric deformation and allows effective analysis of soil deformations under shallow foundations with accurate estimates of settlement, vertical deformations, and lateral displacement profiles, shown by in the two analysed case studies were acurately modelled using the oedometric-continuous corrected law. The continuous equations makes this method suitable for numerical analysis.

7 REFERENCES

Balasubramaniam, A. S., Cai, H., Zhu, D., Surarak, C., & Oh, E. Y. (2010). Settlements of Embankments in Soft Soils. Geotechnical Engineering Journal of the SEAGS & AGSSEA, 41(2), 1-19. Retrieved from http://hdl.handle.net/10072/40431

Balasubramaniam, A., Huang, M., Bolton, M., Oh, E. Y., Bergado, D. T., & Phienwej, N. (2007). Interpretation and analysis oftest embankments in soft clays with and without ground improvement. Geotechnical Engineering Journal of the SEAGS & AGSSEA, 38(3), 235-254. Retrieved from http://hdl.handle.net/10072/16582

Briaud, J. L., & Gibbens, R. (1997). Large-scale load tests and data base of spread footings on sand. McLean, Virginia: Federal Highway Administration, HNR 10.

Briaud, J. L., & Gibbens, R. (1999). Behavior of five large spread footings in sand. Journal of Geotechnical and geoenviromental Engineering, 125(9), 787-796. doi:10.1061/(asce)1090-0241(1999)125:9(787).

Butterfield, R. (1979). A natural compression law for soils (an advance on e-logP'). Géotechnique 29(4), 469–480. doi:10.1680/geot.1979.29.4.469 .

Carneiro, R. F., Gerscovich, D. M., & Danziger, B. R. (2018). Reconstructing edometric compression curves for selecting design parameters. Canadian Geotechnical Journal, 56(5), 621-635. doi:https://doi.org/10.1139/cgj-2018-0018

Chen, L., Gao, Y., Elsayed, A., & Yang, X. (2019). Soil consolidation and vacuum pressure distribution under prefabicatted vertical drains. Geotechnical and Geological Engineering., doi:10.1007/s10706-019-00822-3 .

Da Fonseca, A., Fernandes, M., & Cardoso, A. (1997). Interpretation of a footing load test on a saprolitic soil from granite. Géotechnique, 47(3), 633-651. doi:10.1680/geot.1997.47.3.633 .

Eggestad, A. (1964). Deformation measurements below a model footing on the surface of dry sand. Norwegian Geotechnical Institute Publication, 58, 29-35.

Indraratna, B., Balasubramaniam, A., & Sivaneswaran, N. (1997). Analysis of settlement and lateral deformation of soft clay foundation beneath two full-scale embankments. International Journal for Numerical and Analytical Methods in Geomechanics, 599-618. doi:10.1002/(sici)1096-9853(199709)21:9<599::aid-nag885>3.0.co;2-l

Indraratna, B., Zhong, R., Fox, P., & Rujikiatkamjorn, C. (2017). Large-strain vacuum-assisted consolidation with non-darcian radial flow incorporating varying permeability and compressibility. Journal of Geotechnical and Geoenviromental Engineering, 143(1), (040160880)-1-9. doi:10.1061/(ASCE)GT.1943-5606.0001599

Janbu, N. (1963). Soil compressibility as determined by oedometer and triaxial test. European conference on soil mechanics and foundation engineering, 1, pp. 19-25. Weisbaden, Alemania.

Janbu, N. (1969). The resistance concept applied to deformations of soil. In Proceedings of the 7th International Conference on Soil Mechanics and Foundation Engineering, 1, pp. 191-196. Mexico.

Lambe, T. W., & Marr, W. A. (1979). Stress path method: second edition. Journal of Geotechnical and Geoenvironmental Engineering, 105(6), 727-738.

Loganathan, N., Balasubramaniam, A. S., & Bergado, D. T. (1993). Deformation analysis of enmbankments. Journal of Geotecnical Engineering, 119(8), 1185-1206. doi:10.1061/(asce)0733-9410(1993)119:8(1185)

Mesri, G., & Choi, Y. K. (1985). Settlement Analysis of Embankments on Soft Clays. Journal of Geotechnical Engineering, 111 (4), 441–464. doi:10.1061/(asce)0733-9410(1985)111:4(441)

Nagaraj, T. S., Murthy, B. R., Vatsala, A., & Joshi, R. C. (1990). Analysis of Compressibility of Sensitive Soils. Journal of Geotechnical Engineering, 116(1), 105–118. doi:10.1061/(asce)0733-9410(1990)116:1(105)

Naime, W. (2003). Leyes de comportamiento edométrico de los suelos. Caracas: Trabajo de Ascenso -Agragado UCV.

Naime, W. (2019). Ley Edométrica-Continua para el comportamiento esfuerzo-deformaciónón de los suelos. Revista de la Facultad de IngenieríaUCV, 34(3) . doi:http://saber.ucv.ve/ojs/index.php/rev_fiucv/article/view/20078

Papadopoulos, B. (1992). Settlements of shallow foundations on cohesionless soil. Journal of Geotechnical Engineering, 18(3), 377-393. doi:doi:10.1061/(asce)0733-9410(1992)118:3(377)

Peck, R., & Uyanik, M. (1955). Observed and computed settlements of structures in Chicago. University of Illinois Egineering Experiment Station. Bulletin N° 429, 1-60.

Pitt, J. (1981). Deformation restraint and the mechanics of soil behavior. Iowa State University: Retrospective Theses and Dissertations. doi:https://doi.org/10.31274/rtd-180813-5181.

Schmertmann, J. H. (1953). Estimating the true consolidation behaviour of clay from laboratory test results. Proceedings American Society of Civil Engineers, 79, Issue 10, 1-26.

Schmertmann, J. H., Hartman, J. P., & Brown, P. R. (1978). Improved Strain Influence Factor Diagrams. Journal of Geotechnical and Geoenvironmental Engineering, 104(8), 1131-1135.

Skempton, A. W., Peck, R., & MacDonald, H. (1955). Settlement analyses of six structures in Chicago and London, 4(4). Proceedings of the Institution of Civil Engineers, 525-542.

Sridharan, A., & Gurtug, Y. (2005). Compressibility characteristics of soils. Geotech Geol Eng, 23(5), 615–634. doi:https://doi.org/10.1007/s10706-004-9112-2

Stamatopoulos, A., & Kotzias, P. (1973). The specific constrained modulus. Eighth International Conference of Soil Mechanics and Foundations Engineering, (pp. 1/61-397). Moscow.

Stamatopoulos, A., & Kotzias, P. (1978). Soil compressibility as measured in the oedometer. Géotechnique, 28(4), 363-375. doi.org/10.1680/geot.1978.28.4.363.

Tavenas, F., & Leroueil, S. (1980). The behaviour of embankments on clay foundations. Canadian Geotechnical Journal, 17(2), 236-260. doi:10.1139/t80-025

Tavenas, F., Mieussens, C., & Bourges, F. (1979). Lateral displacements in clay foundations under embankments. Canadian Geotechnical Journal, 16(3), 532-550. doi:10.1139/t79-05

Vesic, A. S., & Clough, G. W. (1968). Behavior of granular materials under high stresses. Journal of Soil Mechanics & Foundations Div, 94(3), 661–668.

Wijemunige, p., & Moh, Z. C. (1989). Trial embankment with stage loading and vertical drains. In Proc., Int. Symp. on Trial Embankments on Malaysian Marine Clays, 2, pp. (26)1-11. Kuala Lumpur, Malaysia.

Wissa, A., Christian, J., Davis, E., & Heiberg, S. (1971). Consolidation at constant rate of strain. Journal of the Soil Mecahnics and Foundation Division, 97(10), 1393-1413.

Yune, C., & Olgun, G. (2016). Effect of layering on total consolidation settlement of normally consolidated clay in 1D conditions. Journal of Geotecnical and Geoenviromental Engineering, 142(2), 06015015 1-5. doi:10.1061/(asce)gt.1943-5606.0001415.

Zheng, J., Hryciw, R. D., & Ventola, A. (2017). Compressibility of Sands of Various Geologic Origins at Pre crushing Stress Levels. Geotechnical and Geological Engineering, 35(5), 2037-2051. doi:10.1007/s10706-017-0225-9